INSTITUTE OF PHYSICS PUBLISHING JOURNAL OF PHYSICS B: ATOMIC, MOLECULAR AND OPTICAL PHYSICS

J. Phys. B: At. Mol. Opt. Phys. **36** (2003) 4107–4126 PII: S0953-4075(03)64572-4

Plasma effect on tunnelling, charge transfer and transient quasimolecular states

D V Fisher[1]

Faculty of Physics, Weizmann Institute of Science, Rehovot 76100, Israel

E-mail: fndima@plasma-gate.weizmann.ac.il

Received 9 June 2003
Published 9 October 2003
Online at stacks.iop.org/JPhysB/36/4107

Abstract

The influence of a dense plasma environment on electron tunnelling between two ion potential wells in collectivized states and in charge-transfer collisions is studied. We show that the tunnelling probabilities in dilute plasma (in a close ion–ion collision) and in dense plasma differ strongly. The difference is due to the mixing between Stark components of donor-ion energy levels, caused by the field of spectator ions in a dense plasma. The mixing is determined by an angle α between the nearest-neighbour ion field and the total electric field acting on the donor ion. In close ion–ion binary collisions the mixing may be considered weak. However, for most plasma ions charge transfer, electron state collectivization and transient quasimolecule formation are strongly affected by the field of spectator ions. We derive approximate analytical expressions for the distribution function of α in an ideal plasma and perform molecular dynamics simulations to find the distribution function of α in both ideal and nonideal plasmas. Both α-dependent and average mixing coefficients are determined. We have found that the mixing is strong, even in ideal plasmas, and increases further with an increase in plasma nonideality. It is shown that there is no resonant charge transfer in dense plasmas. The applicability of a transient 'dicenter' quasimolecule model for dense plasmas is discussed.

1. Introduction

Tunnelling escape of an optical electron from an atom (or ion) into a potential well of a neighbouring ion has been studied extensively for many decades (see, e.g., these monographs [1–4]). These studies show that charge transfer (CT) due to electron tunnelling in an ion–ion collision may have high probability, thus being among the mechanisms that determine the time evolution of plasma ionization composition and populations of quantum states. CT also provides an important tool for plasma diagnostics [4, 5]. Tunnelling-associated phenomena such as

[1] Present primary address: Soreq NRC, Yavneh 81800, Israel.

0953-4075/03/204107+20$30.00

the reduction of effective statistical weights of bound electron states [6–10], ESC [6, 10, 11] and the formation of transient quasimolecular states [12–19] become increasingly important with an increase in plasma density. Tunnelling is also one of the important mechanisms of population and depopulation of collectivized electron states in dense plasmas [11].

When the distance between neighbouring native ions in a plasma becomes comparable to (i.e. not much larger than) the average radius of an optical electron state of one of the ions, that state becomes collectivized. An electron in a collectivized state is confined to potential wells of two or more adjacent ions, in contrast to a true bound state that is confined to a single ionic potential well. A collectivized electron spreads between the potential wells either by tunnelling or above the locally lowered barrier peak. We stress the fact that the distances between individual neighbouring ions in a plasma are not identical and thus any state is collectivized only for a fraction of ions [10].

Until recently, the tunnelling in plasma has been studied exclusively in the two-ion approximation, i.e. only the potentials of the donor ion and the acceptor ion were considered, while the potentials of the surrounding plasma ions and free electrons were neglected. This neglect is reasonable in dilute plasmas (e.g. in crossed-ion-beam or folded-ion-beam experiments [3, 20]) where the characteristic distance between plasma ions is much larger than the average radius of the optical electron wavefunction and CT occurs in relatively rare close heavy-particle collisions. In dense plasmas, however, the *characteristic* distance between ions is not much larger than the average radii of even deep-lying bound states of an optical electron and the applicability of the two-ion approximation becomes limited. In [21] it was shown that the account of an effect of surrounding plasma ions on a two-ion quasimolecule provides better modelling of spectral line profiles in strongly coupled plasmas. In [10, 22] it has been shown that the physical picture of tunnelling and the values of tunnelling rates change radically when the potential of the surrounding plasma particles is accounted for. This strong effect is caused primarily by breaking of the axial symmetry of a two-ion potential by the field of surrounding ions. This symmetry breaking results in mixing between the Stark components of the optical-electron energy level.

In [10] the perturbing potential acting on a test ion has been decomposed into three parts: (i) nearest-neighbour (NN) ion potential, (ii) the ensemble average of the total potential of the other perturbing particles (OPP) and (iii) the stochastic deviations of the total OPP potential from its average value. Term (iii) was further decomposed into an ion (low-frequency) and an electron (high-frequency) components. Term (i) is the one considered in the traditional two-ion, or 'dicenter', approximation. In the traditional approximation terms (ii) and (iii) are not considered. Term (ii) describes plasma polarization (Coulomb screening), i.e. the collective effect of the surrounding particles on the electron states of the test ion. The influence of this term on the tunnelling probability was investigated in [10]. Term (ii) was found to facilitate substantially electron tunnelling between the test ion and its NN ion. The high-frequency component of term (iii), produced by individual free electrons, is largely responsible for level broadening and inelastic transitions. Level broadening and inelastic transitions induced by free electrons are considered in great detail in the monograph [4]. In the present paper we are interested in the effect of the ion component of term (iii). The ions, other than the test ion and its NN ion, are referred to as spectator ions.

2. Charge transfer in dilute and in dense plasma

As we said in the introduction, electron tunnelling between ion potential wells in a plasma affects both the electron state structure (via ESC) and the electron state populations (via the changes in electron-impact and radiative transition probabilities brought along by the ESC,

see [11], and via CT processes). Of course, the timescales involved in ESC, in collectivized state population and depopulation, and in CT are quite different. The characteristic time governing CT is determined by the ion relative velocity and CT interaction range and it is generally assumed that the probability for another (unrelated) kinetic process to occur in one of the interacting ions during that time, and thus to interfere with the CT process, is low. For ESC, on the other hand, the picture of a bound-electron wavefunction changing adiabatically in the field of an approaching NN ion and tunnelling into its potential well is inapplicable. It has been shown [11] that the collectivized states reach population equilibrium with the positive-energy free-electron states on the timescales defined primarily by the long-range electron–electron collisions. On these timescales ions can be considered immobile. In other words, electrons enter and leave the collectivized states *not* due to ion relative motion (as would have been the case if CT between a donor ion and NN ion was involved) but mostly due to electron impact. Note that tunnelling CT to or from *spectator* ions not encompassed by a collectivized state contributes to population and depopulation of that state, and so do radiative processes, too. ESC affects, therefore, the electron state spectrum and transition probabilities between the states [11], but not the populations of the states directly.

In dilute plasmas, CT is important since it affects the populations of the deep-lying energy levels, while only the shallow-lying (i.e. weakly bound) energy levels are collectivized for an appreciable fraction of plasma ions. In dense plasmas, however, the situation is more complicated since the deep-lying energy levels, and sometimes even the ground state, are collectivized for a non-negligible fraction of ions. Still, CT occurs in such plasmas, although it is quite unlikely to affect the population of the native-ion energy levels. The ion-beam ionization-stage composition is affected by CT though, and for such a situation the ESC in native ions and the CT between the native ions and the beam ions must be considered concomitantly.

For the treatment of tunnelling in plasmas the two-ion approximation was traditionally used. In that approximation, electron tunnelling between the potential wells of two ions (donor ion and acceptor ion) is considered and an effect of the surrounding particles is disregarded. As follows from the above discussion, the applicability of the two-ion approximation to the ESC problem, or even to the CT problem in dense plasmas, is questionable.

Let us consider CT in dilute plasmas first. In the cases when CT is considered, one is typically interested in ionization or neutralization of a test ion that penetrates into the plasma bulk. The mean free path of such an ion with respect to CT collision is much larger than the characteristic distance between the native plasma ions. We denote the charge of dominant native ions by Z_i and the test ion charge by Z_t. We denote by R_crit the maximum value of the impact parameter at which the CT is still effective, so that at the given relative ion velocity v the total cross-section for the CT process is $\pi R_\mathrm{crit}^2(v)$. One then easily finds the ratio between the mean free path l_mfp and the characteristic interionic distance

$$a = \left(\tfrac{4}{3}\pi n_\mathrm{i}\right)^{-1/3}$$

to be given by

$$\frac{l_\mathrm{mfp}}{a} = \frac{1}{\pi R_\mathrm{crit}^2 n_\mathrm{i} a} = \frac{4}{3}\left(\frac{a}{R_\mathrm{crit}}\right)^2,$$

where n_i is a number density of the native ions. The condition $l_\mathrm{mfp} \gg a$ is thus equivalent to $R_\mathrm{crit}^2 \ll a^2$. The characteristic electric field F_NN produced by the NN ion at the test ion location during the CT collision between them is $F_\mathrm{NN} \approx Z_\mathrm{i} e/R_\mathrm{crit}^2$, while a characteristic perturbing field produced by *spectator* ions is roughly $F_\mathrm{spec} \approx Z_\mathrm{i} e/a^2 \approx F_0$. Here F_0 is the Holtsmark normal field strength, see [23]. The ratio $F_\mathrm{NN}/F_\mathrm{spec}$ is therefore approximately

equal to $l_{\rm mfp}/a \gg 1$. In experiments measuring CT cross-section this ratio is of the order of 10^5 or larger[2]. Thus the typical perturbing field is at least five orders of magnitude smaller than the NN ion field that causes the CT. Here it is presumed, of course, that the electron state of the donor ion (and thus also $R_{\rm crit}$) remains unchanged along the donor-ion flight path until the CT collision. Thus, in dilute plasmas, i.e. in plasmas with $a \gg R_{\rm crit}$, the traditional two-ion approximation is indeed applicable.

The relation $F_{\rm NN}/F_{\rm spec} \gg 1$ may, in principle, be violated in an improbable case when the next-nearest-neighbour (NNN) ion—a spectator ion—is located at the distance $\rho \ll a$ from the test ion at the time when the CT process occurs. However, using the expressions (7)–(9) of [26] one finds that even in the ideal plasmas the probability of simultaneously finding two ions at the distance $\rho \ll a$ or closer from the test ion is proportional to $(\rho/a)^6$. In nonideal plasmas this probability is further suppressed exponentially due to the Coulomb repulsion between the test ion and the neighbour ions. This suppression is important even in weakly coupled plasmas [26]. Thus, for the CT process the probability of finding a spectator ion at a distance $\rho \ll a$ from either the donor or acceptor ion is negligible.

For the collectivized electron states in plasmas the situation is quite different. There, one is *a priori* interested in the case of $R_{\rm crit}$ comparable to a, since the distribution function for the distance r to the NN ion in plasmas (and in nonideal plasmas in particular) has a rather sharp maximum in the vicinity of $r \approx a$, see [26], and therefore most 'dicenters' found in plasmas at any instant have the centre separation approximately equal to a. The typical values of the distance to the perturbing neighbouring ions (such as, for example, the distance ρ to the NNN ion) are comparable to r, see [26] for a detailed discussion. Therefore, for transient quasimolecular states $F_{\rm spec}$ is, on average, not much smaller than $F_{\rm NN}$. Indeed, in plasmas with the ion–ion coupling parameter

$$\Gamma_{\rm ii} = \frac{Z_{\rm i}^2 e^2}{aT} \tag{1}$$

in the range $0 \leqslant \Gamma_{\rm ii} < 1$, the typical values of the ratio $F_{\rm NN}/F_{\rm spec}$ are between 1 and 2. We have found by molecular dynamics (MD) simulations[3] the average value $\langle F_{\rm NN}/F_{\rm spec}\rangle \approx 1.90$ for weakly coupled plasmas ($\Gamma_{\rm ii} \ll 1$). In nonideal plasmas with $Z_{\rm i} = 1$, MD simulations yield $\langle F_{\rm NN}/F_{\rm spec}\rangle \approx 1.61$ for $\Gamma_{\rm ii} \approx 0.44$ and $\langle F_{\rm NN}/F_{\rm spec}\rangle \approx 1.50$ for $\Gamma_{\rm ii} \approx 0.83$.

It is important to stress that the spectator-ion field $F_{\rm spec}$ can*not* be considered uniform on the size scale a of the quasimolecule, since the few NN ions are located at typical distances of only (1–2)a from the quasimolecule centre. For example, the average absolute value

$$\Delta F_{\rm spec} = \langle |\mathbf{F}_{\rm spec}(\mathbf{r}_{\rm A}) - \mathbf{F}_{\rm spec}(\mathbf{r}_{\rm B})| \rangle$$

of the difference between $\mathbf{F}_{\rm spec}$ vectors at the locations $\mathbf{r}_{\rm A}$ and $\mathbf{r}_{\rm B}$ of the ions A and B comprising the quasimolecule, *in the cases when not only* B *is the NN ion for* A *but also* A *is the NN ion for* B, is comparable to $Z_{\rm i}e/a^2$. For ideal plasmas we have found $\Delta F_{\rm spec} \approx 1.16\ Z_{\rm i}e/a^2$. Furthermore, when B is the NN ion for A, it is not at all necessary that A is the NN ion for B. That is, one or more spectator ions can be located closer to B than the ion A. In fact, in the ideal plasmas in approximately 41% of cases A is *not* the NN ion for B when B is the NN ion for A. In such cases it is not possible to claim that A and B form a 'dicenter' quasimolecule at all, see [22].

[2] For CT cross-sections measured in tokamaks, see [24]. In these experiments, the ion density is $\sim 10^{13}$ cm^{-3} and the largest cross-sections measured are a few times 10^{-14} cm^2. For beam–beam or beam–gas CT cross-section measurements, the ratio $(a/R_{\rm crit})^2$ is much larger yet. Ion densities in beams used to measure CT cross-sections are $\sim 10^6$–10^8 cm^{-3} (see [3, 25]), while the largest cross-sections measured are $\sim 10^{-13}$ cm^2, yielding $(a/R_{\rm crit})^2 \gtrsim 10^8$. Note that neutral atoms (e.g. in beam–gas experiments) contribute neither to $F_{\rm spec}$ nor to a.

[3] For the details of simulations see [10, 26].

The above observations have important implications not only on the tunnelling process, as will be shown further on, but also on the CT in dense plasmas in general. The presence of the considerable local fields changing significantly on the length scale of the order of a implies that even the CT occurring between two *identical* parent ions in dense plasmas[4] is *not* a resonant process. Indeed, each of these two ions is immersed into a different local environment and their respective energy levels do not coincide. Therefore, the CT interaction between two ions A^{+j} and B^{+k} (which may be of the same kind) occurs differently in dilute plasmas and in dense plasmas. In dilute plasmas CT can be described quite accurately as an interaction between the two ions involved:

$$A^{+j} + B^{+k} \rightarrow A^{+(j+i)} + B^{+(k-i)}, \tag{2}$$

where i is the number of electrons being transferred and j and k are the respective initial ionization degrees. In dense plasmas, however, the fields of the surrounding charged particles affect substantially the wavefunctions of the electrons being transferred and therefore the correct interaction scheme is

$$A^{+j}E_1 + B^{+k}E_2 \rightarrow A^{+(j+i)}E_1' + B^{+(k-i)}E_2', \tag{3}$$

where E_1 and E_2 are the local environments of the ions A and B, respectively (i.e. the spectator ions surrounding A and B, and a screening free-electron background). Therefore, CT between two ions in a dense plasma is similar to the interaction between two different *molecules* rather than to the interaction between two isolated ions. We stress that, although the ions $A^{+(j+i)}$ and B^{+k} may be identical, the 'molecules' $A^{+(j+i)}E_1'$ and $B^{+k}E_2$ are certainly different (indeed, there is an infinite variety of spatial arrangements of perturber ions around a given ion) and the CT process is certainly nonresonant. The difference in the cross-sections of the resonant versus nonresonant CT can be very large; see, for example, [3]. As a consequence, the results obtained for the CT cross-sections in dilute plasmas (i.e. in the pair interaction of individual ions at $R_{\rm crit} \ll a$) can*not* be applied to CT in dense plasmas. Likewise, the traditional two-ion approximation, applicable to tunnelling CT in dilute plasmas, cannot be utilized for dense plasma studies. For tunnelling in dense plasmas, as occurs in CT collisions and in collectivized states, one must take into account the effect of the spectator ions.

3. Effects of the surrounding particles

We consider the effect of the stochastic part of the electric field of spectator ions in plasmas on the process of tunnelling of the test-ion optical electron into the potential well of its NN ion. The transfer of one electron only is considered. We identify the donor ion (the ion losing an electron by tunnelling) as the test ion for the purpose of describing the spatial distribution of ions surrounding it. $Z_{\rm t}$ denotes the test ion charge prior to the tunnelling electron loss. The NN ion, i.e. the ion nearest to the test ion, is identified as the acceptor ion. Tunnelling probability drops rapidly with interionic distance: thus it is highly unlikely that an ion other than the NN ion would serve as an acceptor. The plasma is considered dense, in the sense that $R_{\rm crit}$ is comparable to a. The energy level n of the test-ion optical electron is not necessarily the ground state. In fact, the study of electron tunnelling escape from excited states in a dense plasma is crucial for a proper determination of the plasma composition and properties (see [10, 11]).

[4] We reiterate that the distinction between the 'dense plasma' and the 'dilute plasma' is drawn here according to the relation of the $R_{\rm crit}/a$ ratio to unity, namely $R_{\rm crit}/a \ll 1$ in dilute plasmas while $R_{\rm crit}/a$ is comparable to 1 in dense plasmas.

In the absence of the plasma environment, the problem of electron tunnelling between two Coulomb potential wells has been treated in detail, see [2, 27]. It should be emphasized that the treatment of the ion potentials as Coulomb, in the context of tunnelling, does not necessarily mean that the test ion is hydrogen-like or that its NN ion is fully ionized. For now we assume that the splitting of the optical-electron energy level n into Stark components (in the field of the NN ion) is significantly larger than the splitting of the level n into the angular-momentum components nl (due to the effect of the core electrons in an isolated test ion), i.e. that the Stark effect in the NN ion field is linear. Generalization is provided later in this section. The presence of the core electrons in the test ion manifests itself simply in the change of the optical-electron binding energy E_b with respect to its pure Coulomb value $(Z_t + 1)^2 e^2/2n^2$. Consequently, the effective principal quantum number n^* is introduced using

$$E_b = \frac{e^2}{2}\left(\frac{Z_t + 1}{n^*}\right)^2,$$

see [10]. The presence of the core electrons in the NN ion is insignificant as long as the density of states (DOS) available to the tunnelling electron in the NN ion potential well may be considered large (see [2]). This is likely to be the case in dense plasmas, since there the tunnelling is one of the mechanisms of ESC between several ions (see the discussion in [10]) and thus for tunnelling in dense plasmas the DOS at the energy considered is larger than the corresponding DOS in a potential well of the isolated NN ion.

We emphasize here the fact that a dense plasma environment changes significantly the DOS for the tunnelling electron. There seem to be four significant quantum-mechanical mechanisms affecting the optical electron DOS. The first mechanism is the shift and splitting of the energy levels in the field of spectator ions (see, e.g., [4]). The second mechanism is the screening of ionic potentials by the free electrons (see [10, 21]). The third mechanism is the increase in the number of available states due to the possibility for an electron to move or tunnel further into additional ion wells. As we said, the distance-to-NN-ion distribution in dense plasmas has a rather sharp maximum in the vicinity of a. Therefore, there is a high probability that another ion is approximately as close to the NN ion as the NN ion is to the test ion. This way, chains of potential wells accessible for the test-ion optical electron may form. The DOS increases with the number of accessible ion wells. In the limit when 'the ion cluster percolates' (see [28]), i.e. when the number of ion wells accessible for the optical electron (either by an overbarrier escape or by tunnelling, see the discussion in [10]) becomes large, one can expect the individual energy levels to form a conductivity band, in which the *total* DOS (per unit energy) is proportional to the number of ions involved. Finally, the fourth mechanism is the electron impact broadening of the energy levels (see, e.g., [4]). The joint action of these mechanisms tends to increase the average DOS value at the tunnelling electron energy. This implies that the domain of applicability of the tunnelling approximation to the CT problem in dense plasmas is significantly broader than is demarcated in [2] for CT in two-ion collisions.

Let us now return to the effect of spectator ions in dense plasmas on the tunnelling proper. The stochastic part of the field of spectator ions produces two significant effects on the potential in which the tunnelling occurs, see [10]. The first effect is the rotation of the local field direction away from the axis connecting the test ion and its NN ion. This causes mixing between the Stark components of the energy level of the tunnelling electron. The second effect is the distortion of the two-ion potential. This effect either facilitates or hinders the tunnelling, depending on the direction of the perturbing field. *In this paper we focus on the first of the two effects, since it seems to be the dominant one* [10].

Physics of the mixing effect of spectator ions on Stark components of the level n of the test-ion optical electron (and, consequently, on the tunnelling of that electron into the potential

well of the NN ion) was described in [10, 22]. The $2n^2$-fold degeneracy[5] of the level n in an isolated test ion is partially removed in a plasma by an existence of a nonzero electric field $\mathbf{F}$ at the test-ion location. The local electric field $\mathbf{F} = \mathbf{F}_{\rm NN} + \mathbf{F}_{\rm spec}$ is a sum of the NN-ion field $\mathbf{F}_{\rm NN}$ and the field $\mathbf{F}_{\rm spec}$ of spectator ions. The Stark components of the level n of the test ion, from which the tunnelling occurs, are, to a good approximation, eigenstates of the test ion in the total field $\mathbf{F}$ at the test-ion location. This means that in a parabolic-coordinates representation the z axis is chosen along $\mathbf{F}$. However, the probability of tunnelling is governed not by the wavefunction amplitudes in the parent-ion potential well, but rather by the wavefunction behaviour along the tunnelling path, close to the direction connecting the test ion and its NN ion (which is the direction of $\mathbf{F}_{\rm NN}$). In the idealized two-ion picture, applicable to the CT process in dilute plasmas, one finds $\mathbf{F} = \mathbf{F}_{\rm NN}$, the z axis is directed along the least-action tunnelling path and therefore tunnelling from pure Stark components is considered. In dense plasmas, however, $\mathbf{F}$ and $\mathbf{F}_{\rm NN}$ are not parallel and therefore the Stark component states are rotated in space with respect to the tunnelling path. This means that the tunnelling occurs not from the pure Stark components, but rather from their superpositions defined, to a good approximation, by the spatial rotation of the Stark state wavefunctions by the angle α between the directions of $\mathbf{F}$ and $\mathbf{F}_{\rm NN}$, see figure 1 of [22]. This mixing reduces differences in tunnelling probabilities between the components of the same energy level, and thus results in much higher tunnelling probabilities from the components from which, in the pure two-ion case, the tunnelling is slowest. (Namely, the components localized the furthest away from the NN ion and the components with a high absolute value of angular momentum z-projection.)

Another way to look at the same effect is as follows. As long as the only external source of electric field at the donor ion location is the NN ion, the only chosen direction is that towards the NN ion, coinciding with the least-action tunnelling path. Consequently, the projection m of optical-electron angular momentum on the least-action tunnelling path is conserved (we neglect the spin–orbit interaction). The energy level components with $m \neq 0$ have zero amplitude all along the least-action tunnelling path [29]. Therefore tunnelling probabilities for these components are notably lower than for the $m = 0$ component of the same level. In the presence of the spectator electric field, that is not collinear with the least-action tunnelling path, m is no longer conserved and no component has zero amplitude all along that path. Therefore, in a plasma environment the tunnelling probability discrimination against $m \neq 0$ components is removed and the tunnelling probabilities from those components are much higher in the presence than in the absence of a plasma environment. *This is true both for energy levels that exhibit linear Stark effect and for the energy levels that do not.*

The rest of this paper is structured as follows. In section 4 we give the expressions for the mixing coefficients as functions of the rotation angle α. In sections 5 and 6 we study the distribution function of $\cos\alpha$ in ideal and nonideal plasmas, respectively. In section 7 we present the characteristic (averaged) values of the mixing coefficients. In section 8 we summarize the results presented and draw conclusions.

Below we introduce three distribution functions for $\cos\alpha$. The distribution function $P_\alpha(\cos\alpha)$ is the exact distribution function of $\cos\alpha$ in plasmas with given macroscopic parameters (chemical composition, ion density and temperature). The fitting function $P_\alpha^{\rm fit}(\cos\alpha)$ is an analytical expression providing a least-squares fit to $P_\alpha(\cos\alpha)$ in the weak coupling limit. The approximate distribution function $\tilde{P}_\alpha(\cos\alpha)$ is the distribution function of $\cos\alpha$ in plasmas with given macroscopic parameters, obtained in the approximation that replaces the total field of the surrounding ions (besides the NN ion) by the field of the NNN ion alone. The expression for $\tilde{P}_\alpha(\cos\alpha)$ in the weak coupling limit is derived analytically in section 5.1.

[5] Or approximate degeneracy, in the presence of core electrons and/or relativistic corrections.

4. Mixing coefficients

We consider first a level exhibiting a linear Stark effect in the NN ion field. Let $|n_1, n_2, m\rangle$ be the Stark components of a level n of the donor ion in the field $\mathbf{F}_{\rm NN}$ of its NN ion alone. We consider the mixing between these components brought along by the spectator field $\mathbf{F}_{\rm spec}$. We denote by $\mathbf{F}$ the total field, $\mathbf{F} = \mathbf{F}_{\rm NN} + \mathbf{F}_{\rm spec}$, at the donor-ion location. We consider only the linear Stark effect, neglecting the higher-order contributions. In this limit, the optical electron energy eigenstates are the Stark component states $|\nu_1, \nu_2, \mu\rangle$ in the total field $\mathbf{F}$. The wavefunctions $\langle \mathbf{r}|\nu_1, \nu_2, \mu\rangle$ do not depend on the field strength $F = |\mathbf{F}|$. They do, however, depend on the direction of the field. Thus, in the total field $\mathbf{F}$ the Stark component wavefunctions are rotated in space with respect to their form $\langle \mathbf{r}|n_1, n_2, m\rangle$ in the field $\mathbf{F}_{\rm NN}$ alone. The angle of rotation α is, of course, the angle between the directions of the fields $\mathbf{F}$ and $\mathbf{F}_{\rm NN}$. The rotated states notation ν_1, ν_2, μ is chosen in such a way that $\nu_1, \nu_2, \mu \to n_1, n_2, m$ when $\alpha \to 0$.

The matrix elements of the rotation operator $\hat{\Phi}(\eta \equiv \cos\alpha)$ in the subspace of the Stark components of level n are readily found. The two vectors, $\mathbf{F}$ and $\mathbf{F}_{\rm NN}$, define a plane in space. We denote it as the yz plane. The rotation is then around the x axis. To determine the matrix elements $\langle n_1', n_2', m'|\hat{\Phi}(\eta)|n_1, n_2, m\rangle$ it is simplest to move from a parabolic to spherical representation of the Coulomb system bound states. Both the transformation coefficients $\langle n_1, n_2, m|l, m\rangle$, given by Clebsch–Gordan coefficients, and the matrix elements of the finite-angle rotation operator around the x axis $\langle l', m'|\hat{\Phi}(\eta)|l, m\rangle \sim \delta_{l,l'}$ are given, for example, in [29]. The matrix elements therefore can be simply written as

$$A^{n_1,n_2,m}_{\nu_1,\nu_2,\mu}(\eta) \equiv \langle \nu_1, \nu_2, \mu|\hat{\Phi}(\eta)|n_1, n_2, m\rangle$$
$$= \sum_{l=\max\{|m|,|\mu|\}}^{n-1} \langle \nu_1, \nu_2, \mu|l, \mu\rangle\langle l, \mu|\hat{\Phi}(\eta)|l, m\rangle\langle l, m|n_1, n_2, m\rangle.$$

The probability of tunnelling Γ from a state which is a mixture of Stark components of the same manifold contains no interference terms [2, 27, 30]. Thus, for the rates of tunnelling we simply obtain

$$\Gamma_{\nu_1,\nu_2,\mu}(\eta) = \sum_{n_1,n_2,m} |A^{\nu_1,\nu_2,\mu}_{n_1,n_2,m}|^2 \Gamma_{n_1,n_2,m}. \tag{4}$$

For the energy levels that have a large splitting on l and do not exhibit a linear Stark effect in the NN ion field, mixing may be assumed to occur only within individual nl levels. (This is an estimate only, since in the external field l is not conserved.) Tunnelling probabilities are then given directly by

$$\Gamma_{n,l,\mu}(\eta) = \sum_m |\langle l, \mu|\hat{\Phi}(\eta)|l, m\rangle|^2 \Gamma_{n,l,m}.$$

Of course, for $\Gamma_{n,l,m}$ evaluation the linear Stark term in expression (20) of [27] must be omitted. For additional effects of the plasma environment on tunnelling probabilities see section 4.5 of [10].

In many cases it is important to know the characteristic degree of mixing, averaged over the ensemble, rather than the mixing coefficient values $|A|^2$ for a certain rotation angle α. Averaging over the ensemble implies here averaging over the distribution $P_\alpha(\eta)\,\mathrm{d}\eta$ of the rotation angle cosine, $\eta = \cos\alpha$, in a plasma. Indeed, every spatial arrangement of ions around a donor ion produces a certain value of η. We define the characteristic values $C^{\nu_1,\nu_2,\mu}_{n_1,n_2,m}$ of the mixing coefficients by averaging the absolute value squared of the matrix elements over the η distribution:

$$C^{\nu_1,\nu_2,\mu}_{n_1,n_2,m} = \int_{-1}^{1} |A^{\nu_1,\nu_2,\mu}_{n_1,n_2,m}|^2 P_\alpha(\eta)\,\mathrm{d}\eta. \tag{5}$$

The distribution function $P_\alpha(\eta)$ cannot be derived analytically for a general case of the local perturbing field $\mathbf{F}_{\rm spec}$ produced by many spectator ions in a nonideal plasma. However, the largest contribution to the local perturbing field in a plasma is provided by the field $\mathbf{F}_{\rm NNN}$ of the NNN ion. We denote the distribution function of η in the approximation $\mathbf{F}_{\rm spec} = \mathbf{F}_{\rm NNN}$ by $\tilde{P}_\alpha(\eta)$. For an ideal plasma, the distributions of the distance and the angle to the NNN ion are known [26] and it is therefore possible to derive the ideal-plasma $\tilde{P}_\alpha(\eta)$ analytically. The weak coupling (i.e. ideal-plasma) limit of $\tilde{P}_\alpha(\eta)$ is denoted by $\tilde{P}^{\rm id}_\alpha(\eta)$. We derive the expression for $\tilde{P}^{\rm id}_\alpha(\eta)$ in section 5.1. In section 5.2 we report the ideal-plasma MD simulations of the exact distribution function $P^{\rm id}_\alpha(\eta)$ free from the $\mathbf{F}_{\rm spec} = \mathbf{F}_{\rm NNN}$ approximation. For nonideal plasmas, we present a theoretical analysis and MD simulation results for $\tilde{P}_\alpha(\eta)$ and $P_\alpha(\eta)$ in section 6.

5. Rotation angle distribution in ideal plasmas

5.1. Mixing produced by the next-nearest-neighbour ion

Here we approximate $\mathbf{F}_{\rm spec}$ by the field of the NNN ion, $\mathbf{F}_{\rm spec} = \mathbf{F}_{\rm NNN}$. Let us denote by θ the angle between the vectors $\mathbf{F}_{\rm NN}$ and $\mathbf{F}_{\rm spec}$ at the donor-ion location. It is easy to see that the relation between the angles α and θ is given by

$$\cos\alpha(\cos\theta, \xi^2) = \frac{\xi^2 + \cos\theta}{\sqrt{\xi^4 + 2\xi^2\cos\theta + 1}}, \tag{6}$$

where $\xi^2 = F_{\rm NN}/F_{\rm NNN}$. We denote the acceptor (i.e. the NN ion) charge by $Z_{\rm A}$, and the NNN ion charge by $Z_{\rm NNN}$. Then, one finds $\xi^2 = k\zeta^2$, where $\zeta = \rho/r \geqslant 1$ is the ratio of distances to the NNN and NN ions, respectively, and $k = Z_{\rm A}/Z_{\rm NNN} \geqslant 1$. The probability $\tilde{P}^{\rm id}_\alpha(\eta)\,{\rm d}\eta$ to find the $\eta = \cos\alpha$ value within the interval $(\eta, \eta + {\rm d}\eta)$ can now be obtained analytically. Indeed, denoting the probability to find $\chi = \cos\theta$ within a given interval $(\chi, \chi + {\rm d}\chi)$ by $P_\theta(\chi)\,{\rm d}\chi$ and the probability to find ζ within the interval $(\zeta, \zeta + {\rm d}\zeta)$ by $P_{\rm rat}(\zeta)\,{\rm d}\zeta$, we identify

$$\tilde{P}^{\rm id}_\alpha(\eta) = \int_{-1}^{1} {\rm d}\chi\; P_\theta(\chi) \int_1^\infty {\rm d}\zeta\; P_{\rm rat}(\zeta)\delta\{\eta - \cos\alpha(\chi, k\zeta^2)\}. \tag{7}$$

Here the absence of a correlation between χ and ζ in an ideal plasma is utilized. In nonideal plasmas $P_{\rm rat}(\zeta)$ is, strictly speaking, a function of χ. Taking the ideal plasma distribution functions $P_{\rm rat}(\zeta) = 3\zeta^{-4}$ and $P_\theta(\chi) = 1/2$, see [26], the integration (7) can be carried out. It yields

$$\tilde{P}^{\rm id}_\alpha(\eta) = \begin{cases} \dfrac{3}{4}k^{3/2}\displaystyle\int_{\chi_{\rm min}}^{\chi_{\rm max}} {\rm d}\chi\; \frac{(\xi_0^4 + 2\xi_0^2\chi + 1)^{3/2}}{\xi_0^5(1-\chi^2)} & \text{for } \sqrt{1-k^{-2}} \leqslant \eta \leqslant 1, \\ 0 & \text{for } \eta \leqslant \sqrt{1-k^{-2}}, \end{cases} \tag{8}$$

where we have denoted

$$\xi_0(\chi) = \left\{\eta\left(\frac{1-\chi^2}{1-\eta^2}\right)^{1/2} - \chi\right\}^{1/2}, \tag{9}$$

$$\chi_{\rm min} = -k(1-\eta^2) - \eta\{1 - k^2(1-\eta^2)\}^{1/2}, \tag{10}$$

$$\chi_{\rm max} = -k(1-\eta^2) + \eta\{1 - k^2(1-\eta^2)\}^{1/2}. \tag{11}$$

Note that $\tilde{P}^{\rm id}_\alpha(\eta)$ has a mild singularity at the edge of the η domain:

$$\lim_{\eta\to 1} \tilde{P}^{\rm id}_\alpha(\eta) \sim (1-\eta)^{-1/4}. \tag{12}$$

This is due to the power-law (rather than exponential) decay of the function $P_{\rm rat}(\zeta)$ at large ζ in ideal plasmas. Indeed, for large values of ζ we have $\alpha \to 0$, i.e. $\eta \to 1$, regardless of the

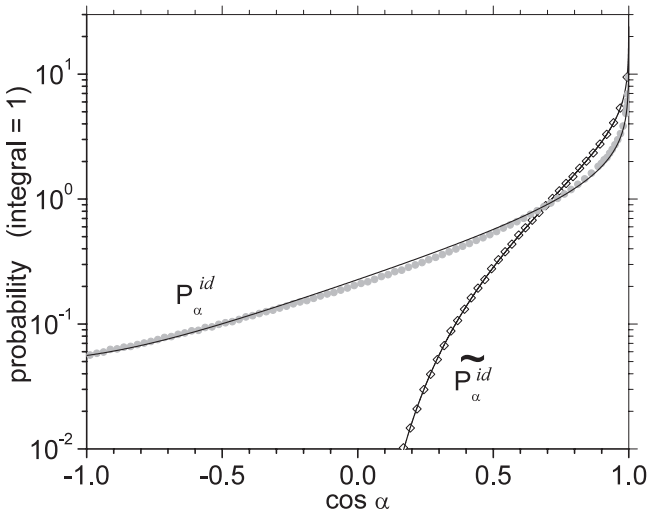

Figure 1. Distribution functions of $\cos\alpha = \mathbf{F}\cdot\mathbf{F}_{\rm NN}/FF_{\rm NN}$ in an ideal plasma. The MD simulation results for $\tilde{P}^{\rm id}_\alpha(\cos\alpha)$ and $P^{\rm id}_\alpha(\cos\alpha)$ are shown by empty and full symbols, respectively. Thick full curves show the theoretical prediction (13) for the distribution $\tilde{P}^{\rm id}_\alpha(\cos\alpha)$ and the fitting function $P^{\rm fit}_\alpha(\cos\alpha)$ approximating the distribution $P^{\rm id}_\alpha(\cos\alpha)$.

value of χ. As we explain below, in nonideal plasmas this singularity is removed, no matter how weak the nonideality is.

As expected, in an ideal plasma the distribution $\tilde{P}_\alpha(\eta)$ does not depend on $Z_{\rm t}$ but depends on $k = Z_{\rm A}/Z_{\rm NNN}$. For nonideal plasmas the dependence on $Z_{\rm t}$ emerges, due to the dependence on $Z_{\rm t}$ of the distribution of χ and ζ in nonideal plasmas. For $Z_{\rm A} = Z_{\rm NNN}$, which is the most common case in dense plasmas, one finds $k = 1$ and thus

$$\tilde{P}^{\rm id}_\alpha(\eta) = \begin{cases} \dfrac{3}{4}\displaystyle\int_{-1}^{-1+2\eta^2} {\rm d}\chi\, \frac{(\xi_0^4 + 2\xi_0^2\chi + 1)^{3/2}}{\xi_0^5(1-\chi^2)} & \text{for } 0 \leqslant \eta \leqslant 1, \\ 0 & \text{for } \eta \leqslant 0. \end{cases} \tag{13}$$

5.2. Mixing produced by all the surrounding ions: MD simulations

In plasmas, the perturbing local-ion field $\mathbf{F}_{\rm spec}$ is produced not only by the NNN ion, but rather by all the spectator ions within several Debye radii from the donor ion. The perturbing field $F_{\rm spec}$ is, in this case, not necessarily weaker than $F_{\rm NN}$. Thus, α can now exceed $\pi/2$, i.e. $P_\alpha(\eta) > 0$ for $\eta \leqslant 0$, in contrast to $\tilde{P}_\alpha(\eta)$ which is zero for negative η.

In order to find the distribution function $P_\alpha(\eta)$ we have conducted a series of MD simulations. Details of the simulation method were described in [26]. Local microfields were simulated by superposition of Coulomb fields of electrons and ions within the test volume. Both electrons and ions were taken to be point-like. The electron–ion interaction was regularized at short distances in order to avoid Coulomb collapse. No model potentials were used in MD simulations at any stage. All the plasma ions were taken to have the same charge, i.e. $Z_{\rm A} = Z_{\rm NNN} = Z_{\rm i}$. Simulations were conducted both for ideal plasmas (straight-line particle trajectories) and for nonideal plasmas (classical mechanics particle trajectories). Results of the latter are discussed in the next section. The distribution function $P^{\rm id}_\alpha(\eta)$ we have found in ideal plasmas is shown in figure 1. For comparison, the function $\tilde{P}^{\rm id}_\alpha(\eta)$ is also

shown in the same figure. One can see that the simulated curve for $\tilde{P}_\alpha^{\rm id}(\eta)$ coincides with the theoretical curve given by expression (13) above, thus providing a good test for the MD simulation accuracy. Figure 1 also shows the ideal plasma fitting curve for $P_\alpha^{\rm id}(\eta)$. The fitting curve equation (15) is presented below.

We note that, in order to ensure high accuracy of the MD simulation results for **F**, the number of ions simulated simultaneously was 8000 or higher (up to 1.575×10^5) for an ideal plasma. For nonideal plasmas, 1260 electrons plus 1260 ions were simultaneously simulated. We have found that, even for ideal plasmas, 1260 ions in the simulated volume were sufficient to simulate the distribution function $P_\alpha(\eta)$ with a relative systematic error of about 10% or smaller. For nonideal plasmas the relative systematic error caused by the finite number of ions is smaller yet, due to the Debye screening which effectively limits the ion–ion interaction range. For the distribution function $\tilde{P}_\alpha^{\rm id}(\eta)$ and for its generalization to nonideal plasmas $\tilde{P}_\alpha(\eta)$ only the fields of the NN and NNN ions affect the value of η. Therefore, the relative systematic error caused by the finite number of ions is negligible for $\tilde{P}_\alpha(\eta)$ and $\tilde{P}_\alpha^{\rm id}(\eta)$.

The distribution function $P_\alpha(\eta)$ has a sharp peak at $\eta \to 1$, similar to $\tilde{P}_\alpha(\eta)$. This is expected, since the peak at $\eta \to 1$ is produced by close approaches between the NN ion and the donor ion. Then $F_{\rm NN} \gg F_{\rm spec}$ and one finds $\eta \to 1$ for any values of $F_{\rm spec}$ and θ, no matter whether $F_{\rm spec}$ is produced by all the perturber ions or by the NNN ion alone. The asymptotic behaviour of $P_\alpha^{\rm id}(\eta)$ at $\eta \to 1$ is similar to that of $\tilde{P}_\alpha^{\rm id}(\eta)$, namely

$$\lim_{\eta \to 1} P_\alpha(\eta) \sim (1-\eta)^{-1/4}. \tag{14}$$

However, the proportionality constants in expressions (12) and (14) differ. The expression (14) is derived in the appendix.

Note that, although both the distribution $P_\alpha(\eta)$ and the distribution $\tilde{P}_\alpha(\eta)$ have a peak at $\eta \to 1$, the probability distribution $P(\alpha)$ of the *angle* α (where $\cos\alpha = \eta$) has no peak at $\alpha \to 0$. In fact, the probability $P(\alpha)$, given by $P(\alpha)\,{\rm d}\alpha = P_\alpha(\cos\alpha)\sin\alpha\,{\rm d}\alpha$, tends to *zero* at $\alpha \to 0$. This means that the chance to find the vectors **F** and $\mathbf{F}_{\rm NN}$ within an acute angle $\alpha \ll 1$ from each other tends to zero faster than α. Namely, in an ideal plasma

$$\int_0^{\alpha \ll 1} P(\alpha')\,{\rm d}\alpha' \sim \alpha^{3/2},$$

and in a nonideal plasma, where $P_\alpha(\eta)$ is finite at $\eta = 1$,

$$\int_0^{\alpha \ll 1} P(\alpha')\,{\rm d}\alpha' \sim \alpha^2.$$

To make possible the use of the distribution $P_\alpha^{\rm id}(\eta)$ in practical calculations, we have fitted the simulated curve in figure 1 by a semi-empirical expression:

$$P_\alpha^{\rm fit}(\eta) = A(1-\eta)^{-0.25} + B + C(1-\eta) + D(1-\eta)^\Delta. \tag{15}$$

We used the least-squares minimization under the constraint

$$\int_{-1}^{1} P_\alpha^{\rm fit}(\eta)\,{\rm d}\eta = 1.$$

The best-fitting set of parameter values was found by fixing $A = 1.80$. The values of the fitting parameters were then found to be given by

$$\begin{aligned} A &= 1.80, \\ B &= 53.358\,94, \\ C &= 0.240\,6642, \\ D &= -55.172\,76, \\ \Delta &= 3.268\,027 \times 10^{-3}. \end{aligned} \tag{16}$$

6. Rotation angle distribution in nonideal plasmas

In nonideal plasmas, the Coulomb interaction between individual particles affects the local spatial ion distribution functions. These effects were studied in detail in [26]. Here we utilize the results reported in [26] to study the changes in the distribution function $P_\alpha(\eta)$ with an increase in the plasma ion–ion coupling parameter Γ_{ii}, equation (1).

It is worthwhile considering first the changes that occur in the *approximate* distribution function $\tilde{P}_\alpha(\eta)$ obtained approximating $\mathbf{F}_{spec} = \mathbf{F}_{NNN}$. By definition, $\tilde{P}_\alpha(\eta) \to \tilde{P}_\alpha^{id}(\eta)$ in the limit $\Gamma_{ii} \to 0$. A qualitative change occurs in $\tilde{P}_\alpha(\eta)$ when Γ_{ii} becomes nonzero. This change is due to the different asymptotic behaviour of the function $P_{rat}(\zeta)$ at large ζ for $\Gamma_{ii} = 0$ and for $\Gamma_{ii} > 0$. As explained in [26], the power-law tail of the distribution $P_{rat}(\zeta)$ for $\Gamma_{ii} = 0$ is due to the possibility of a close approach between the donor ion and the NN ion in strictly ideal plasmas. For $\Gamma_{ii} > 0$, the large-ζ asymptotic decay of $P_{rat}(\zeta)$ is always exponential. As a result, the singularity in $\tilde{P}_\alpha(\eta)$ at $\eta \to 1$, present for $\Gamma_{ii} = 0$, vanishes when the plasma nonideality is taken into account. Nevertheless, even for $\Gamma_{ii} \sim 1$ the function $\tilde{P}_\alpha(\eta)$ has a maximum at $\eta \to 1$.

Another nonideality effect influencing the $\tilde{P}_\alpha(\eta)$ distribution is the decrease in the $P_\theta(\chi)$ distribution in the region $\chi \approx 1$ as Γ_{ii} increases [26]. The decrease in $P_\theta(\chi)$ is due to the repulsion between the NN and NNN ions, which is strongest at $\chi \to 1$. In the limit $\chi = 1$ one finds $\eta = 1$ for any ζ value. Thus, the decrease in $P_\theta(\chi \to 1)$ causes an additional reduction in $\tilde{P}_\alpha(\eta \to 1)$.

The same nonideality effects influence the shape of the *exact* distribution function $P_\alpha(\eta)$, too. The dominant nonideality effect is produced by the short-range (i.e. unscreened) Coulomb ion–ion repulsion. The probability of a close approach between the donor ion and the NN ion decreases with Γ_{ii}, thus reducing the probability of finding $F_{NN} \gg F_{spec}$. This results in a reduction of the peak of $P_\alpha(\eta \to 1)$. As is said above, the $(1-\eta)^{-1/4}$ singularity in $P_\alpha(\eta)$ at $\Gamma_{ii} = 0$ is removed at $\Gamma_{ii} > 0$ by the short-range ion–ion repulsion. As another result of the Coulomb ion–ion repulsion, the next-nearest ions are less likely to concentrate in the vicinity of the NN ion in nonideal plasmas, i.e. the probability for $\mathbf{F}_{spec}$ and $\mathbf{F}_{NN}$ to be nearly collinear decreases with Γ_{ii}. This effect also leads to a reduction of the peak of $P_\alpha(\eta)$ at $\eta \to 1$ with an increase in Γ_{ii}.

For the sake of completeness we note that, for the exact distribution function $P_\alpha(\eta)$, not in all local configurations in which $F_{NN} \gg F_{spec}$ does one find $r^2 \ll a^2$. In a certain fraction of configurations with $F_{NN} \gg F_{spec}$, one finds $r \approx a$, and $F_{spec} \ll Ze/a^2$ due to cancellation between the electric fields of individual perturber ions[6]. This fraction is insignificant in an ideal plasma. However, it increases with Γ_{ii} and becomes significant in nonideal plasmas, $\Gamma_{ii} \sim 1$, since the probability of finding $r^2 \ll a^2$ decreases rapidly with Γ_{ii} (see [26]) whereas the probability of finding $F \ll Ze/a^2$ increases with Γ_{ii} (see section 4.3 of [4]). The probability of finding $F_{spec} \ll Ze/a^2$ also increases with Γ_{ii} up to a certain Γ_{ii} value (larger than unity) at which the short-range order becomes important. The configurations with $F_{NN} \gg F_{spec}$ correspond to $\eta \to 1$. Therefore the cancellation described here acts to enhance the peak of $P_\alpha(\eta)$ at $\eta \to 1$ with an increase in Γ_{ii}, in contrast to the two effects described above.

For even higher Γ_{ii} the vectors $\mathbf{F}_{NN}$ and $\mathbf{F}_{spec}$ tend to become of the order of Ze/a^2 and antiparallel. In the limit $\Gamma_{ii} \gg 1$ ions settle into a crystal lattice. Then, the probability of finding $r^2 \ll a^2$ tends to zero and the probability of finding $F \ll Ze/a^2$ tends to unity, so in all likelihood $F = |\mathbf{F}_{NN} + \mathbf{F}_{spec}| \ll F_{NN} \approx F_{spec}$ for $\Gamma_{ii} \gg 1$. However, here we are interested

[6] Likewise, the possibility of cancellation of individual ion fields results in a substantial probability of finding $F_{NN} \gg F$ even though $F_{NN} \lesssim F_0$. This fact has some highly nontrivial physical consequences, as explained in [10].

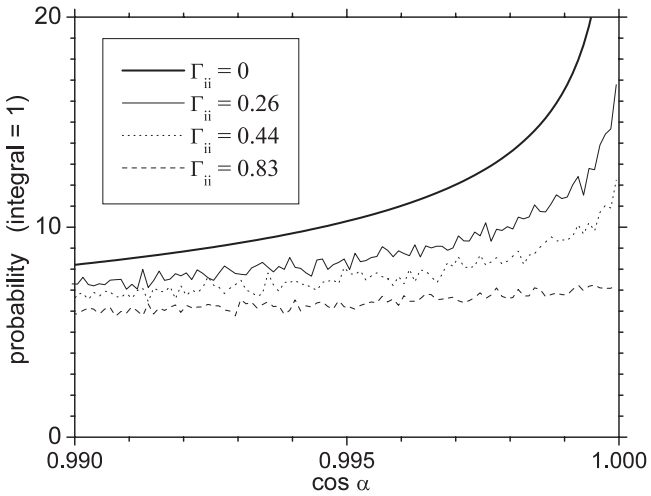

Figure 2. Distribution function $\tilde{P}_\alpha(\cos\alpha)$ shown in the peak region ($\cos\alpha \approx 1$) for several values of Γ_{ii}. The thick full curve shows the analytical result for $\Gamma_{ii} = 0$, equation (13). Thin curves show the MD simulation results. The lowest line ($\Gamma_{ii} = 0.83$) should be regarded as a qualitative result only, since, as explained in [26], the present MD simulations provide good accuracy for Γ_{ii} values of roughly 0.5 or lower.

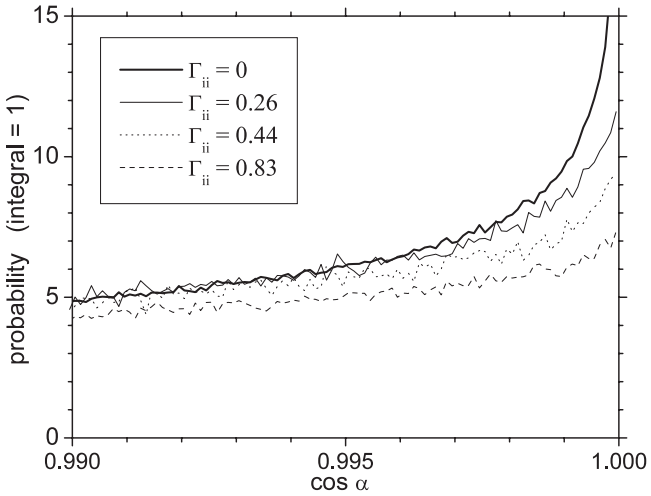

Figure 3. Distribution function $P_\alpha(\cos\alpha)$ shown in the peak region ($\cos\alpha \approx 1$) for several values of Γ_{ii}. All curves are produced by MD simulations. Here, as in figure 2, the $\Gamma_{ii} = 0.83$ curve should be regarded as a qualitative result only.

in the $\cos\alpha$ distribution only for $\Gamma_{ii} \lesssim 1$. Indeed, for $\Gamma_{ii} > 1$ the distances to the nearest spectator ions (e.g. to the NNN ion) is almost identical to the distance to the NN ion and the distribution of $\cos\alpha$ does not describe properly the perturbation produced by the spectator ions anymore.

In figures 2 and 3 we present the MD simulation results for the functions $\tilde{P}_\alpha(\eta)$ and $P_\alpha(\eta)$, respectively, in the vicinity of the $\eta = 1$ limit, for several values of Γ_{ii}. One can see that the prominent peak of the η distribution at $\eta \to 1$ is decreasing substantially with Γ_{ii}, as predicted.

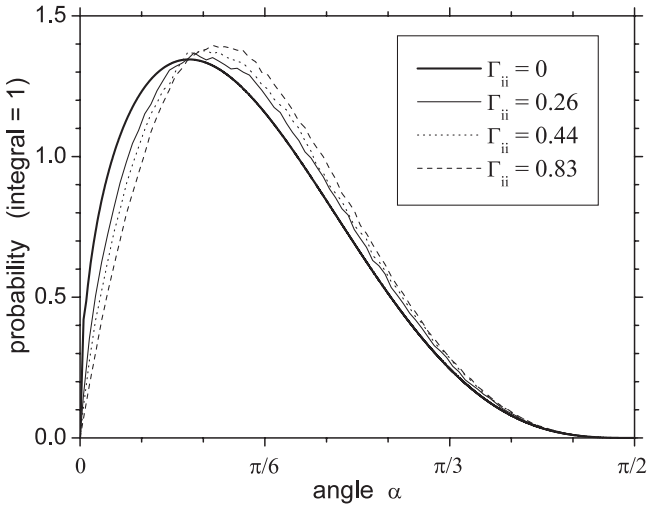

Figure 4. Distribution function $\tilde{P}_\alpha(\cos\alpha)\sin\alpha$ shown for several values of Γ_{ii}. The thick full curve shows the analytical result for $\Gamma_{ii} = 0$, equation (13). Thin curves show the MD simulation results.

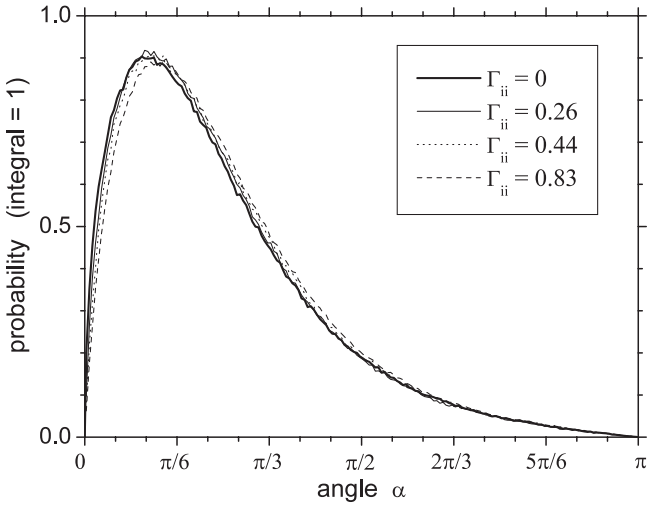

Figure 5. Distribution function $P_\alpha(\cos\alpha)\sin\alpha$ shown for several values of Γ_{ii}. All curves are produced by MD simulations.

This effect is especially pronounced for $\tilde{P}_\alpha(\eta)$. We remind that the distribution function $\tilde{P}_\alpha(\eta)$ is defined using the approximation $F_{\mathrm{spec}} = F_{\mathrm{NNN}}$, and thus it contains no contribution to the $\eta \to 1$ peak from the cancellation in F_{spec} while, as explained above, this cancellation contributes significantly to the $\eta \to 1$ peak of $P_\alpha(\eta)$ at $\Gamma_{ii} \sim 1$. This fact explains the greater sensitivity of $\tilde{P}_\alpha(\eta)$ than of $P_\alpha(\eta)$ to the increase in Γ_{ii}.

In figures 4 and 5 we present the MD simulation results for the functions $\tilde{P}_\alpha(\eta)$ and $P_\alpha(\eta)$, respectively, in the form of distributions of the angle α. The probabilities of finding the angle value between α and $\alpha + \mathrm{d}\alpha$ are given by $\tilde{P}_\alpha(\cos\alpha)\sin\alpha\,\mathrm{d}\alpha$ and $P_\alpha(\cos\alpha)\sin\alpha\,\mathrm{d}\alpha$, respectively. Note that, although $0 \leqslant \alpha \leqslant \pi$, the distribution $\tilde{P}_\alpha(\cos\alpha)\sin\alpha$ in figure 4 is shown for $0 \leqslant \alpha \leqslant \pi/2$ only, as $\tilde{P}_\alpha$ is identically zero at $\pi/2 \leqslant \alpha \leqslant \pi$ for $Z_{\mathrm{A}} = Z_{\mathrm{NNN}}$.

7. Average mixing coefficient values

We have calculated the characteristic values of the mixing coefficients squared, $C^{\nu_1,\nu_2,\mu}_{n_1,n_2,m}$, in an ideal plasma using an analytic approximate distribution $\tilde{P}^{\rm id}_\alpha(\eta)$, expression (13), in (5). The calculations were repeated using the fitted exact ideal plasma η distribution $P^{\rm fit}_\alpha(\eta)$, expression (15), in (5). The calculation results show the existence of strong mixing.

For the distribution $\tilde{P}^{\rm id}_\alpha(\eta)$ the following results were found. The typical absolute value squared of the diagonal elements, $C^{n_1,n_2,m}_{n_1,n_2,m}$, is in the range 0.49–0.69 for $n = 4$, in the range 0.22–0.51 for $n = 8$, and in the range 0.13–0.41 for $n = 12$. The typical values of the off-diagonal mixing coefficient squares $C^{\nu_1,\nu_2,\mu}_{n_1,n_2,m}$ decrease slowly with an increase in $|\nu_1 - n_1|$, $|\nu_2 - n_2|$ and $|\mu - m|$, from the typical values of 10^{-1}–10^{-2} to the minimal values of the order of $10^{-n}n$. The tunnelling probabilities of the pure Stark states, on the other hand, are very sensitive [27, 30, 31] to the value of $n_2 - n_1$. Therefore, it turns out that, for the Stark components with the largest value of $n_2 - n_1$, for which in the absence of mixing the tunnelling probabilities were by far the highest, the tunnelling probabilities decrease typically by less than a factor of 2. At the same time, for the components with large values of $n_1 - n_2$, for which in the absence of mixing the tunnelling probabilities were many orders of magnitude lower, the mixing leads to a drastic increase in the tunnelling probabilities.

For the fitted accurate distribution $P^{\rm fit}_\alpha(\eta)$ the mixing, as expected, was found to be somewhat stronger still. The off-diagonal mixing coefficients were found to be larger in this case and the diagonal elements somewhat smaller. The decrease in the tunnelling probability of the fastest-decaying component was found to be given approximately by a factor of 2–3 for $n = 2$–10, respectively, while the increase in the tunnelling probabilities of the slower-decaying components, as already said above, is dramatic. The strong mixing effect is thus confirmed.

We have tabulated the values of the mixing coefficients (5) for $2 \leqslant n \leqslant 14$ using the approximate distribution $\tilde{P}^{\rm id}_\alpha(\eta)$, and for $2 \leqslant n \leqslant 13$ using the analytical fit $P^{\rm fit}_\alpha(\eta)$ to the distribution $P_\alpha(\eta)$. The table of $C^{\nu_1,\nu_2,\mu}_{n_1,n_2,m}$ values found using $P^{\rm fit}_\alpha(\eta)$ has been made available on the Internet [32].

As we have shown, for $\Gamma_{\rm ii} < 1$ the peak in the distribution $P_\alpha(\eta)$ at $\eta \to 1$ diminishes with an increase in $\Gamma_{\rm ii}$. The values of $\eta \to 1$ contribute least to the mixing. Therefore the mixing (which we have shown to be strong even in the ideal dense plasmas) becomes stronger still with an increase in plasma nonideality. This trend continues up to $\Gamma_{\rm ii} \approx 1$. In the domain $\Gamma_{\rm ii} > 1$ the typical distances from the test ion to a few nearest-neighbour ions become nearly identical. As a consequence, a strong cancellation emerges in the perturbing field and the peak in $P_\alpha(\eta)$ at $\eta \to 1$ starts to grow with the further increase in $\Gamma_{\rm ii}$. However, at $\Gamma_{\rm ii} > 1$ similarity of the distances to the few closest neighbours renders the distribution $P_\alpha(\eta)$ largely useless.

8. Conclusions

We have carried out a study of the effect of a dense plasma environment on the process of electron tunnelling between two ionic potential wells, and on the CT problem in general. It was shown that the two-ion model is applicable only to the CT collisions in dilute plasmas. The dense plasma environment (and, in particular, the local electric field produced by spectator ions) perturbs significantly the two-ion potential and influences strongly the electron states and the CT process. As a result, even when the donor parent ion and the acceptor ion are identical the CT process in a dense plasma is not resonant. The presence of strong non-uniform fields of spectator ions at the location of the two-ion system necessitates an account of individual spectator ions as a part of the system. That is, a restriction of the transient-quasimolecule

description of a dense plasma to the 'dicenter' approximation does not seem to be justified. It was shown that the tunnelling description of the optical electron transfer between ions in dense plasmas (in a CT process or in a collectivized, quasimolecular state) has a wider range of applicability than the two-ion model suggests and that the tunnelling probabilities are changed dramatically by the effect of the surrounding ions.

Electric fields of the individual spectator ions are found to produce a strong mixing between the Stark components of the donor-ion energy levels. This results in a dramatic increase in the probabilities of tunnelling from the highest-lying Stark components (those components for which, in a two-ion approximation, the tunnelling probabilities are the lowest) and from the components with a relatively large angular momentum component in the acceptor-ion direction. The latter effect occurs also in atoms (ions) that do not exhibit linear Stark splitting in the acceptor-ion field. The mixing coefficient values for any individual donor ion are determined by a single parameter, namely by an electric field rotation angle α. The mixing coefficients were evaluated as functions of α.

We have investigated the distribution function $P_\alpha(\cos\alpha)$ for both ideal and nonideal plasmas. An approximate distribution function $\tilde{P}_\alpha(\cos\alpha)$ in an ideal plasma was derived analytically. MD simulations were performed for the approximate distribution function $\tilde{P}_\alpha(\cos\alpha)$ and for the exact distribution function $P_\alpha(\cos\alpha)$ in both ideal and nonideal plasmas. The dependence of $\tilde{P}_\alpha(\cos\alpha)$ and $P_\alpha(\cos\alpha)$ on the plasma coupling parameter has been studied in detail. We have determined that the mixing increases with an increase in plasma ion–ion coupling parameter up to $\Gamma_{ii} \approx 1$. Finally, characteristic values of the mixing coefficients were found by averaging over the distribution of α.

Present results for the tunnelling ESC were incorporated into a time-dependent collisional–radiative code reported in [11]. We are working on inclusion of the CT process into the code. That will provide a tool for the simulation of emission spectra also for plasmas with level populations affected by CT. Comparison of simulated spectra to experimental ones will then allow for indirect experimental assessment of the present predictions for the probabilities of CT in dense plasmas.

Acknowledgment

The author gratefully acknowledges fruitful discussions with Y Maron.

Appendix. Asymptotic behaviour of $P_\alpha(\eta)$ in an ideal plasma

We denote by $P_{tot}(F)$ the distribution of an absolute value F of the electric field produced at a given location by all the plasma ions, and by $P_{spec}(F_{spec})$ the distribution of an absolute value F_{spec} of the field produced at the same location by the spectator ions (i.e. by all the ions except the NN ion). In an ideal plasma, the spatial distribution of any perturber ion does not depend on the positions of any other ions. Consequently, the field F at any point in space (and, specifically, at the donor ion location) has a Holtsmark distribution:

$$P_{tot}(F)\,\mathrm{d}F = \frac{\mathrm{d}F}{F_0}\,H\left(\frac{F}{F_0}\right),$$

where

$$F_0 = \frac{2\pi}{(5\pi)^{2/3}}\frac{Z_i e}{a^2} \approx \frac{Z_i e}{a^2}. \tag{17}$$

However, the independence of the ion positions does *not* imply that, at the donor-ion location, the distribution $P_{spec}(F_{spec})$ is also Holtsmark. It is easy to show that $P_{spec}(F_{spec})$ differs from

the Holtsmark distribution, using the following construction. We introduce $P^{\rm cond}_{\rm spec}(F_{\rm spec}|r)$, which is the distribution of $F_{\rm spec}$ for a given distance r between the donor ion and the NN ion. By definition

$$P_{\rm spec}(F_{\rm spec}) = \int_0^\infty P^{\rm cond}_{\rm spec}(F_{\rm spec}|r)\,P_{\rm NN}(r)\,{\rm d}r,$$

where $P_{\rm NN}(r)\,{\rm d}r$ is the distribution of the distance to the NN ion, see [26]. In an ideal plasma

$$P_{\rm NN}(r)\,{\rm d}r = 3\frac{r^2\,{\rm d}r}{a^3}\exp\left(-\frac{r^3}{a^3}\right).$$

For any given value of r there are, by definition, no perturber ions closer than r to the donor ion, and therefore the larger r is the smaller the average value of $F_{\rm spec}$ is, which is

$$\langle F_{\rm spec}(r)\rangle \equiv \int_0^\infty F_{\rm spec}\,P^{\rm cond}_{\rm spec}(F_{\rm spec}|r)\,{\rm d}F_{\rm spec}.$$

For $r \to 0$, however, the volume free of ions around the donor ion becomes negligible, and in this limit the distribution $P^{\rm cond}_{\rm spec}(F_{\rm spec}|r)$ approaches the Holtsmark distribution:

$$\lim_{r\to 0} P^{\rm cond}_{\rm spec}(F_{\rm spec}|r) = \frac{1}{F_0}H\left(\frac{F_{\rm spec}}{F_0}\right). \tag{18}$$

It is thus clear that $\langle F_{\rm spec}(r)\rangle$ only approaches the Holtsmark average field $\langle F\rangle$ for $r \to 0$, and $\langle F_{\rm spec}(r)\rangle < \langle F\rangle$ for $r > 0$. Therefore, the average value of $F_{\rm spec}$, given by

$$\langle F_{\rm spec}\rangle \equiv \int_0^\infty \langle F_{\rm spec}(r)\rangle\,P_{\rm NN}(r)\,{\rm d}r,$$

is smaller than the Holtsmark average field $\langle F\rangle$, proving that $P_{\rm spec}(F_{\rm spec}) \neq \frac{1}{F_0}H\left(\frac{F_{\rm spec}}{F_0}\right)$.

The distribution function $P_\alpha(\eta)$ is, in general, determined by

$$P_\alpha(\eta) = \int_0^\infty P_{\rm NN}(r)\,{\rm d}r \int_0^\infty P^{\rm cond}_{\rm spec}(F_{\rm spec}|r)\,{\rm d}F_{\rm spec} \int_{-1}^{1} P_\theta(\cos\theta) \times \delta\{\eta - \cos\alpha(\cos\theta,\, F_{\rm NN}(r)/F_{\rm spec})\}\,{\rm d}(\cos\theta).$$

We are interested in the asymptotic behaviour of $P^{\rm id}_\alpha(\eta)$ at $\eta \to 1$. As is said above, the peak (and, in fact, the mild singularity) in $P^{\rm id}_\alpha(\eta)$ at $\eta \to 1$ appears due to the possibility of the close approach between the NN ion and the donor ion, i.e. due to the relatively slow (power-law) convergence of $P_{\rm NN}(r)$ at $r \to 0$ in ideal plasmas. Thus, the main contribution to $P^{\rm id}_\alpha(\eta)$ in the region $\eta \to 1$ comes from the small-r domain, $0 \leqslant r \ll a$, of the integral on dr above. Choosing an arbitrary constant $r_0 \ll a$ as an upper limit for the integration on dr, we obtain

$$\lim_{\eta\to 1} P^{\rm id}_\alpha(\eta) \approx \int_0^{r_0\ll a} P_{\rm NN}(r)\,{\rm d}r \int_0^\infty P^{\rm cond}_{\rm spec}(F_{\rm spec}|r)\,{\rm d}F_{\rm spec} \int_{-1}^{1} P_\theta(\cos\theta) \times \delta\{\eta - \cos\alpha(\cos\theta,\, F_{\rm NN}(r)/F_{\rm spec})\}\,{\rm d}(\cos\theta). \tag{19}$$

Above we have explained that, in the limit of $r \to 0$ (i.e. $r \ll a$), one can use expression (18) for $P^{\rm cond}_{\rm spec}$. Strictly speaking, expression (18) above is only true for $F_{\rm spec} < Z_{\rm i}e/r^2$, i.e. for the bulk of the $F_{\rm spec}$ distribution but not for the distal part of its tail (note that for $r \ll a$ one finds $Z_{\rm i}e/r^2 \gg Z_{\rm i}e/a^2 \approx F_0$). The tail of the Holtsmark distribution is formed by single-ion close approaches [23]. Therefore, it is accurate to approximate

$$P^{\rm cond}_{\rm spec}(F_{\rm spec}|r \ll a) \approx \begin{cases} \dfrac{1}{F_0}H\left(\dfrac{F_{\rm spec}}{F_0}\right) & \text{for } F_{\rm spec} < Z_{\rm i}e/r^2, \\ 0 & \text{for } F_{\rm spec} \geqslant Z_{\rm i}e/r^2. \end{cases}$$

In the integral (19) we also use

$$P_{\mathrm{NN}}(r \ll a) \approx 3\frac{r^2}{a^3}$$

and

$$P_\theta(\cos\theta) = \tfrac{1}{2}.$$

The last expression is generally true for ideal plasmas, since the directions of $\mathbf{F}_{\mathrm{NN}}$ and $\mathbf{F}_{\mathrm{spec}}$ are not correlated. The expression (19) thus becomes

$$\lim_{\eta\to 1} P_\alpha^{\mathrm{id}}(\eta) \approx \frac{3}{2}\int_0^{r_0}\frac{r^2\,\mathrm{d}r}{a^3}\int_0^{Z_\mathrm{i}e/r^2}\frac{\mathrm{d}F_{\mathrm{spec}}}{F_0}H\left(\frac{F_{\mathrm{spec}}}{F_0}\right) \times\int_{-1}^{1}\delta\left\{\eta-\frac{(Z_\mathrm{A}e/r^2F_{\mathrm{spec}})+\chi}{\sqrt{(Z_\mathrm{A}e/r^2F_{\mathrm{spec}})^2+2(Z_\mathrm{A}e/r^2F_{\mathrm{spec}})\chi+1}}\right\}\mathrm{d}\chi, \tag{20}$$

where we have used the expression (6) for $\cos\alpha(\cos\theta, F_{\mathrm{NN}}(r)/F_{\mathrm{spec}})$ and denoted $\cos\theta = \chi$. Note that the NN ion charge Z_A need not coincide with the characteristic native (spectator) ion charge Z_i.

The order of integration on $\mathrm{d}r$ and on $\mathrm{d}F_{\mathrm{spec}}$ may be changed in the following way:

$$\int_0^{r_0}\frac{r^2\,\mathrm{d}r}{a^3}\int_0^{Z_\mathrm{i}e/r^2}\mathrm{d}F_{\mathrm{spec}}\,f(r,F_{\mathrm{spec}}) = \int_0^{\infty}\mathrm{d}F_{\mathrm{spec}}\int_0^{\min(r_0,\sqrt{Z_\mathrm{i}e/F_{\mathrm{spec}}})}\frac{r^2\,\mathrm{d}r}{a^3}f(r,F_{\mathrm{spec}}),$$

where $f(r, F_{\mathrm{spec}})$ is any integrable function. Denoting $Z_\mathrm{A}e/r^2F_{\mathrm{spec}} = \xi^2$ and observing that

$$\frac{r^2|\,\mathrm{d}r|}{a^3} = \left(\frac{Z_\mathrm{A}e}{a^2F_{\mathrm{spec}}}\right)^{3/2}\frac{|\,\mathrm{d}\xi|}{\xi^4}$$

we find that the above integral becomes

$$\int_0^{\infty}\mathrm{d}F_{\mathrm{spec}}\int_0^{\min(r_0,\sqrt{Z_\mathrm{i}e/F_{\mathrm{spec}}})}\frac{r^2\,\mathrm{d}r}{a^3}f(r,F_{\mathrm{spec}}) = \int_0^{\infty}\mathrm{d}F_{\mathrm{spec}}\left(\frac{Z_\mathrm{i}e}{a^2F_{\mathrm{spec}}}\right)^{3/2}\int_{\xi_m(F_{\mathrm{spec}})}^{\infty}\frac{\mathrm{d}\xi}{\xi^4}f\left(\sqrt{\frac{Z_\mathrm{i}e}{F_{\mathrm{spec}}\xi^2}},F_{\mathrm{spec}}\right),$$

where

$$\xi_m(F_{\mathrm{spec}}) = \max\left(\sqrt{\frac{Z_\mathrm{A}}{Z_\mathrm{i}}},\sqrt{\frac{Z_\mathrm{i}e}{F_{\mathrm{spec}}r_0^2}}\right).$$

Performing this transformation in expression (20) we find

$$\lim_{\eta\to 1} P_\alpha^{\mathrm{id}}(\eta) \approx \frac{3}{2}\int_0^{\infty}\frac{\mathrm{d}F_{\mathrm{spec}}}{F_0}\left(\frac{Z_\mathrm{A}e}{a^2F_{\mathrm{spec}}}\right)^{3/2}H\left(\frac{F_{\mathrm{spec}}}{F_0}\right) \times\int_{-1}^{1}\mathrm{d}\chi\int_{\xi_m(F_{\mathrm{spec}})}^{\infty}\frac{\mathrm{d}\xi}{\xi^4}\,\delta\left\{\eta-\frac{\xi^2+\chi}{\sqrt{\xi^4+2\xi^2\chi+1}}\right\}. \tag{21}$$

The second line of this expression coincides with expression (7), except for a different lower limit of the integration on ξ. However, this difference is unimportant as far as the $\eta \to 1$ limit is concerned, since the singularity is produced by integration in the domain $\xi \gg 1$. Therefore, the second line of (21), and thus the entire expression, is proportional to $(1-\eta)^{-1/4}$. Indeed

$$\int_{-1}^{1}\mathrm{d}\chi\int_{\xi_m}^{\infty}\frac{\mathrm{d}\xi}{\xi^4}\,\delta\left\{\eta-\frac{\xi^2+\chi}{\sqrt{\xi^4+2\xi^2\chi+1}}\right\} = \int_{\xi_m}^{\infty}\frac{\mathrm{d}\xi}{\xi^2}\int_{-\xi^{-2}}^{\xi^{-2}}\mathrm{d}\sigma\,\delta\left\{1-\varepsilon-\frac{1+\sigma}{\sqrt{1+2\sigma+\xi^{-4}}}\right\}, \tag{22}$$

where we have introduced

$$\varepsilon = 1 - \eta$$

and

$$\sigma = \frac{\chi}{\xi^2}.$$

As we said, the principal contribution to the integral in the limit $\varepsilon \to 0$ comes from the $\xi \gg 1$ domain, so $\sigma \sim \xi^{-2} \ll 1$. Preserving only the leading order in ξ^{-2} we expand

$$1 - \varepsilon - \frac{1+\sigma}{\sqrt{1+2\sigma+\xi^{-4}}} \approx \frac{1}{2}(\xi^{-4} - \sigma^2) - \varepsilon.$$

The integration over σ yields then

$$\lim_{(\varepsilon\to 0, \xi \gg 1)} \int_{-\xi^{-2}}^{\xi^{-2}} \mathrm{d}\sigma\, \delta\left\{1 - \varepsilon - \frac{1+\sigma}{\sqrt{1+2\sigma+\xi^{-4}}}\right\} \approx \frac{1}{\sqrt{\xi^{-4} - 2\varepsilon}} \begin{cases} 2 & \text{for } 2\varepsilon \leqslant \xi^{-4} \\ 0 & \text{for } 2\varepsilon > \xi^{-4}, \end{cases}$$

and the entire expression (22) becomes

$$2\int_{\xi_m}^{(2\varepsilon)^{-1/4}} \frac{\mathrm{d}\xi}{\sqrt{1-2\varepsilon\xi^4}} = 2(2\varepsilon)^{-1/4} \int_{\vartheta_{\min}\to 0}^{\pi/2} \frac{\mathrm{d}\vartheta}{\sqrt{1+\sin^2\vartheta}} = 2(2\varepsilon)^{-1/4} \frac{\Gamma^2(\frac{1}{4})}{2^{5/2}\pi^{1/2}},$$

where $\Gamma(x)$ is a gamma function. Here we have replaced $(2\varepsilon)^{1/4}\xi = \sin\vartheta$ and observed that

$$\vartheta_{\min} = \arcsin\left[(2\varepsilon)^{1/4} \max\left(\sqrt{\frac{Z_\mathrm{A}}{Z_\mathrm{i}}}, \sqrt{\frac{Z_\mathrm{i}e}{F_{\mathrm{spec}} r_0^2}}\right)\right] \to 0$$

for $\varepsilon \to 0$. The limit $\varepsilon \to 0$ (i.e. $\eta \to 1$) of the distribution (20) is therefore

$$\lim_{\eta\to 1} P_\alpha^{\mathrm{id}}(\eta) = \frac{3}{2}\frac{\Gamma^2(\frac{1}{4})}{2^{5/2}\pi^{1/2}} 2^{3/4}(1-\eta)^{-1/4} \int_0^\infty \frac{\mathrm{d}F_{\mathrm{spec}}}{F_0} \left(\frac{Z_\mathrm{A} e}{a^2 F_{\mathrm{spec}}}\right)^{3/2} H\left(\frac{F_{\mathrm{spec}}}{F_0}\right).$$

Using equation (17) for F_0, we finally find

$$\lim_{\eta\to 1} P_\alpha^{\mathrm{id}}(\eta) = \frac{15}{16\pi}\frac{\Gamma^2(\frac{1}{4})}{2^{1/4}} \langle\beta^{-3/2}\rangle \left(\frac{Z_\mathrm{A}}{Z_\mathrm{i}}\right)^{3/2} (1-\eta)^{-1/4} \approx 1.755 \left(\frac{Z_\mathrm{A}}{Z_\mathrm{i}}\right)^{3/2} (1-\eta)^{-1/4}, \quad (23)$$

where

$$\langle\beta^{-3/2}\rangle \equiv \int_0^\infty H(\beta)\beta^{-3/2}\,\mathrm{d}\beta \approx 0.5319$$

is the $(-3/2)$th moment of the Holtsmark distribution. Equation (23) gives an *exact* asymptotic form of the distribution of $\eta = \cos\alpha$ in an ideal plasma. We note that the value of the prefactor of $(1-\eta)^{-1/4}$ for $Z_\mathrm{A} = Z_\mathrm{i}$ found by *fitting* the MD results, namely $A = 1.80$ (see equation (16)), is very close to the accurate prefactor value $A = 1.755$.

It is interesting to compare between the exact asymptotic form (23) and the asymptotic form of the *approximate* distribution function $\tilde{P}_\alpha^{\mathrm{id}}(\eta)$ given by equation (8). In the limit $\eta \to 1$ one finds from equations (9)–(11)

$$\chi_{\min} \to -1$$
$$\chi_{\max} \to 1$$
$$\xi_0 \to \left(\frac{1-\chi^2}{2\varepsilon}\right)^{1/4}$$

and

$$\lim_{\varepsilon\to 0}\tilde{P}_{\alpha}^{\mathrm{id}}(\eta\equiv 1-\varepsilon)=\frac{3}{4}\left(\frac{Z_{\mathrm{A}}}{Z_{\mathrm{NNN}}}\right)^{3/2}\int_{-1}^{1}\mathrm{d}\chi\,\frac{\left(1-\chi^2/2\varepsilon\right)^{3/2}}{\left(1-\chi^2/2\varepsilon\right)^{5/4}(1-\chi^2)}$$

$$=\left(\frac{Z_{\mathrm{A}}}{Z_{\mathrm{NNN}}}\right)^{3/2}(1-\eta)^{-1/4}\frac{3}{2^{5/4}}\int_{0}^{1}\frac{\mathrm{d}\chi}{(1-\chi^2)^{3/4}}$$

$$=\frac{3}{4\sqrt{2\pi}}\frac{\Gamma^2(\frac{1}{4})}{2^{1/4}}\left(\frac{Z_{\mathrm{A}}}{Z_{\mathrm{NNN}}}\right)^{3/2}(1-\eta)^{-1/4}\approx 3.307\left(\frac{Z_{\mathrm{A}}}{Z_{\mathrm{NNN}}}\right)^{3/2}(1-\eta)^{-1/4}. \quad (24)$$

Comparing equations (23) and (24), and identifying in the latter the NNN ion as one of the native ions ($Z_{\mathrm{NNN}}=Z_{\mathrm{i}}$), it is easy to see that the functional forms are identical. However, the numerical prefactor is overestimated in the approximate expression (24) by a factor of 1.884.

References

[1] McDowell M R C and Coleman J P 1970 *Introduction to the Theory of Atomic Collisions* (Amsterdam: North-Holland)
[2] Janev R K, Presnyakov L P and Shevelko V P 1985 *Physics of Highly Charged Ions* (Berlin: Springer)
[3] McDaniel E W, Mitchell J B A and Rudd M E 1993 *Atomic Collisions: Heavy Particle Projectiles* (New York: Wiley)
[4] Griem H R 1997 *Principles of Plasma Spectroscopy* (Cambridge: Cambridge University Press)
[5] Lochte-Holtgreven W 1995 *Plasma Diagnostics* (New York: American Institute of Physics)
[6] Gündel H 1970 *Beitr. Plasma Phys.* **10** 455
Gündel H 1971 *Beitr. Plasma Phys.* **11** 1
[7] Zimmerman G B and More R M 1980 *J. Quant. Spectrosc. Radiat. Transfer* **23** 517
[8] Fortov V E and Yakubov I T 1984 *Fizika Neideal'noi Plazmy* (Moscow: IVTAN) (in Russian)
Fortov V E and Yakubov I T 1990 *Physics of Nonideal Plasma* (New York: Hemisphere) (Engl. Transl.)
[9] Seaton M J (ed) 1995 *The Opacity Project* vol 1 (Bristol: Institute of Physics Publishing)
[10] Fisher D V and Maron Y 2002 *Eur. Phys. J.* D **18** 93
[11] Fisher D V and Maron Y 2003 *J. Quant. Spectrosc. Radiat. Transfer* **81** 147
[12] Malnoult P, d'Etat B and Hoe N 1989 *Phys. Rev.* A **40** 1983
[13] Salzmann D, Stein J, Goldberg I B and Pratt R H 1991 *Phys. Rev.* A **44** 1270
[14] Leboucher-Dalimier E, Poquérusse A and Angelo P 1993 *Phys. Rev.* E **47** R1467
[15] Salzmann D 1998 *Atomic Physics in Hot Plasmas* (New York: Oxford University Press)
[16] Sauvan P, Leboucher-Dalimier E, Angelo P, Derfoul H, Ceccotti T, Poquérusse A, Calisti A and Talin B 2000 *J. Quant. Spectrosc. Radiat. Transfer* **65** 511
[17] Oks E 2000 *Phys. Rev. Lett.* **85** 2084
[18] Oks E 2001 *Phys. Rev.* B **63** 057401
[19] Leboucher-Dalimier E, Sauvan P, Angelo P, Poquérusse A, Schott R, Dufour E, Mingues E and Calisti A 2001 *J. Quant. Spectrosc. Radiat. Transfer* **71** 493
[20] Salzborn E 1989 *J. Physique Colloq.* **50** C1 207
[21] Sauvan P, Angelo P, Calisti A, Leboucher-Dalimier E and Mingues E 2001 *J. Quant. Spectrosc. Radiat. Transfer* **71** 675
[22] Fisher D V and Maron Y 2003 *Proc. PNP-11 Conf. (Valencia, March 2003) Contrib. Plasma Phys.* at press
[23] Griem H R 1974 *Spectral Line Broadening by Plasmas* (New York: Academic)
[24] Kato T, Masai K, Fujimoto T, Koike F, Källne E, Marmar E S and Rice J E 1991 *Phys. Rev.* A **44** 6776
[25] Dolder K T 1983 *Physics of Ion–Ion and Electron–Ion Collisions* ed F Brouillard and J W McGowan (New York: Plenum)
[26] Fisher D V and Maron Y 2001 *Eur. Phys. J.* D **14** 349
[27] Grozdanov T P and Janev R K 1978 *Phys. Rev.* A **17** 880
[28] Stein J and Salzmann D 1992 *Phys. Rev.* A **45** 3943
[29] Landau L D and Lifshitz E M 1997 *Quantum Mechanics (Non-Relativistic Theory)* 3rd edn (Wobury, NY: Butterworth-Heinemann)
[30] Fisher D, Maron Y and Pitaevskii L P 1998 *Phys. Rev.* A **58** 2214
[31] Smirnov B M and Chibisov M I 1966 *Sov. Phys.—JETP* **22** 585
[32] http://plasma-gate.weizmann.ac.il/~fndima/mixing/mixing.html